World Academy of Science, Engineering and Technology
International Journal of Physical and Mathematical Sciences
Vol:4, No:11, 2010

Simulation of 3D Flow using Numerical Model at Open-channel Confluences

R.Goudarzizadeh, S.H.Mousavi Jahromi and N.Hedayat

Abstract**—**This paper analytically investigates the 3D flow pattern at the confluences of two rectangular channels having 90^0 angles using Navier-Stokes equations based on Reynolds Stress Turbulence Model (RSM). The equations are solved by the Finite-Volume Method (FVM) and the flow is analyzed in terms of steady-state (single-phased) conditions. The Shumate experimental findings were used to test the validity of data. Comparison of the simulation model with the experimental ones indicated a close proximity between the flow patterns of the two sets. Effects of the discharge ratio on separation zone dimensions created in the main-channel downstream of the confluence indicated an inverse relation, where a decrease in discharge ratio, will entail an increase in the length and width of the separation zone. The study also found the model as a powerful analytical tool in the feasibility study of hydraulic engineering projects.

Keywords**—**90^0 confluence angle, flow separation zone, numerical modeling, turbulent flow.

I. Introduction

CHANNEL confluences are important components of the river networks, the study of which is crucial in the hydraulic engineering. Under conditions where a flow continues in the river network, it has to pass through the confluences. Due to increase in discharge and mixing of flows at a certain point, a zone with a 3D flow pattern having highest turbulence in the river regime is established. This in turn creates scouring and sedimentation at the channel confluence. The results being a significant morphological change in that vicinity which as research [2], [4] suggest can have a fundamental impact on water abstraction from the river in affected zone.

Various studies have been conducted in this respect, one of which is the work of [11] which was based on experiments on a channel junction which produced an equation for the relative depth at the point of confluence. This was developed by [8] who instead investigated the energy loss by classifying it into loss due to roughness and loss due to flow turbulence**.**

The experimental works carried by [1] on a confluence with various angles indicated that by increasing the discharge ratio of the side-channel to the total discharge, the length and width of the separation zone increases. But for different discharge ratios the separation zone shape index (ratio of depth to the separation zone length H/L) remained an average of 0.19.

By assuming that critical depth occurs at the point of high flow velocity, [6] used relations from the continuity, momentum and energy equations to calculate relative depth and coefficient of flow contraction.

[5] Studied a flow junction with various angles where the main-channel width was 500 mm and the side-channel having two different widths of 300 mm and 500 mm. They have presented equations for estimating the dimensions of the flow separation zones under sub-critical and transitory conditions.

[7] Simultaneously used the continuity, momentum and energy equations at a 90^0 confluence to present an equation to calculate flow contraction coefficient (μ) at the point of maximum flow velocity as well as ratio of the upstream depth to downstream (Y).

[10] Used experimental investigations in order to analyze 3D flow at the 90^0 confluence and showed that the separation zone near the water surface have greater length and width. They also found that increase in ratio of the main-channel discharge to the side-channel, the length and width of the separation zone decreases.

The present study is based on the model developed by [10] which calculates the flow velocity by the use of Reynolds Stress Method (RSM) and compared at the results at various sections. The effects of discharge ratio on the dimensions of flow separation zone are also assessed.

II. Materials And Methods

A. The Laboratory Model Specifications

The specifications of the laboratory used in this study are modeled on the channel structures that were originally developed and tested empirically by [8]. The main-channel was designed with a length of 21.946 m (72 ft) and the side-channel having a 3.658 m (12ft). The side-channel in this experiment was situated at 5.486 m (18 ft) downstream of the main-channel entrance. The width that was chosen for the two experimental channels was 0.914 m (3ft).

The distinguishing feature of the experimental channel was in its design configuration that incorporate a horizontal bed at all locations as can be seen in figure 1.

R.Goudarzizadeh, Post-graduate researcher, Islamic Azad University, Dezful Branch, Iran.

S.H.Mousavi Jahromi, Associate professor, S.Chamran University, Ahwaz, Iran.

N.Hedayat, Dean, Faculty of Agriculture, Islamic Azad University, Dezful Branch, Iran.

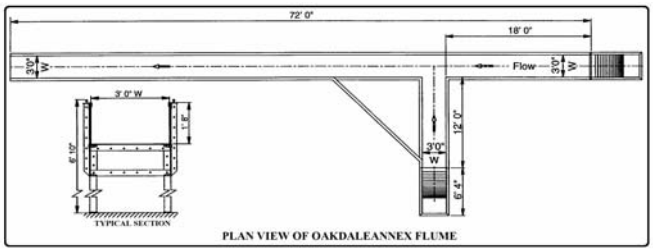

Fig. 1 The laboratory features of the experimental flume

The major experimental parameters consisted of a total discharge assumed at 0.17 m^3/sec (6 f^3/sec) and the downstream depth H_0 fixed at 0.296 m. The average velocity in downstream was then assumed at u_0=0.628 m/sec. The Frude and Reynolds numbers were set at 0.37 and 186000 respectively. The details are shown in table 1.

TABLE I
HYDRAULIC CHARECTERISTICS OF THE COFLUENCE FLOW

Q $(m^3/\sec)$	H_0 (m)	U_0 $(m/\sec)$	F_r	R_e
0.17	0.296	0.628	0.37	186000

B. Governing Equations

The equations used as the theoretical framework for the analysis of open-channel in this experiment consisted of Reynolds-Averaged Navier-Stokes (RANS) that governs the fluid dynamics that are assumed to have incompressible and steady-state characteristics. The steady-state equations (mass continuity) and (momentum) are expressed as follows [9]:

- Continuity equation:

$$\frac{\partial u_i}{\partial x_i} = 0 \tag{1}$$

-Momentum equation:

$$\frac{\partial u_i}{\partial t} + \frac{\partial u_i u_j}{\partial x_j} = -\frac{1}{\rho}\frac{\partial P}{\partial x_i} + g_i + \frac{\partial}{\partial x_j}(\tau_{ij}) \tag{2}$$

This study also incorporated the Finite-Volume Method (FVM) as an analytical framework to discretize the equations.

C. Boundary Conditions

In the main and side-channel inlet, average velocity is adapted. Since the inlet velocity under the laboratory conditions is non-uniform in depth, the length of the main and side-channels should increase in order to establish the appropriate laboratory conditions. An atmospheric pressure is adapted for the outlet with a downstream main-channel of 12 m length.

The boundary conditions of the channel rigid zone are assumed to be wall and from the hydraulic point of view, the surfaces of the channel walls are assumed to be smooth. The variations in water surface are ignored, the symmetry boundary condition for the water surface is applied and the flow depth is H_0=0.296 m which rendered it unnecessary to use the two-phased modeling that is costly. The grid independent test for the size is carried out which ultimately led to a choice of grid with 170×55×27 cells in the main-channel and 45×55×27 cells in the side-channel as is illustrated in figure 2.

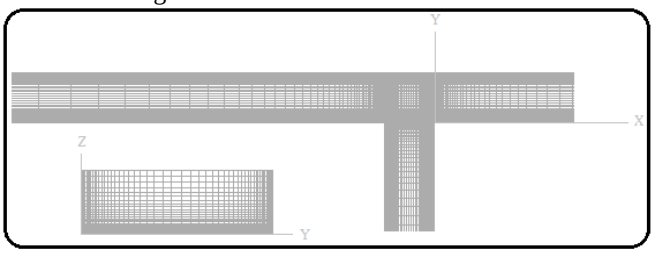

Fig. 2 grid system

The standard wall function is applied here in order to establish a relation between the sub-layer and the fully-turbulent layer.

D. Turbulent Model

By solving the transport equation for the term $\overline{u_i' u_j'}$ the Reynolds Stress Method (RSM) can be arrived at [3]. For the two components *i* and j the momentum equation is deduced from the Navier-Stokes, the outcome of which for the component *i* and *j* are multiplied by the fluctuation velocity u_i' and u_j' respectively. By addition of the two equations and taking timely average from both, the appropriate transport equation for $\overline{u_i' u_j'}$ is arrived at which can be expressed as follows:

$$U_k \frac{\partial \overline{u_i' u_j'}}{\partial x_k} = P_{ij} + \Phi_{ij} + D_{ij} - \varepsilon_{ij} \tag{3}$$

III. RESULTS AND DISCUSSIONS

The velocity profiles in the main-channel reach at various sections are compared with the laboratory results (Fig. 3).

The comparative analysis of the findings suggests a close proximity between the two sets of data and the model's relative high accuracy in forecasting the flow along the longitudinal channel profile. The existence of slight difference in certain regions is rooted in the fact that the flow depth is assumed to be constant. As can be observed from figure 3, the velocity profile at a distance before intersection maintains its developed state ($x/W = 1$) and as approaches the point of flows combination, the velocity profiles, due to the incoming flow from the side-channel, are diverted toward the outer wall of the main-channel ($y/W = 1$). Comparison of the experimental with numerical results at $y/W = 0.75, y/W = 0.875$ (Maximum-velocity zone) and $y/W = 0.125, y/W = 0.25$ (Low-velocity zone) along the main-channel suggests that the numerical results have a close proximity with the experiment ones and the velocity variations

along the main-channel has been properly and appropriately modeled (Fig. 4).

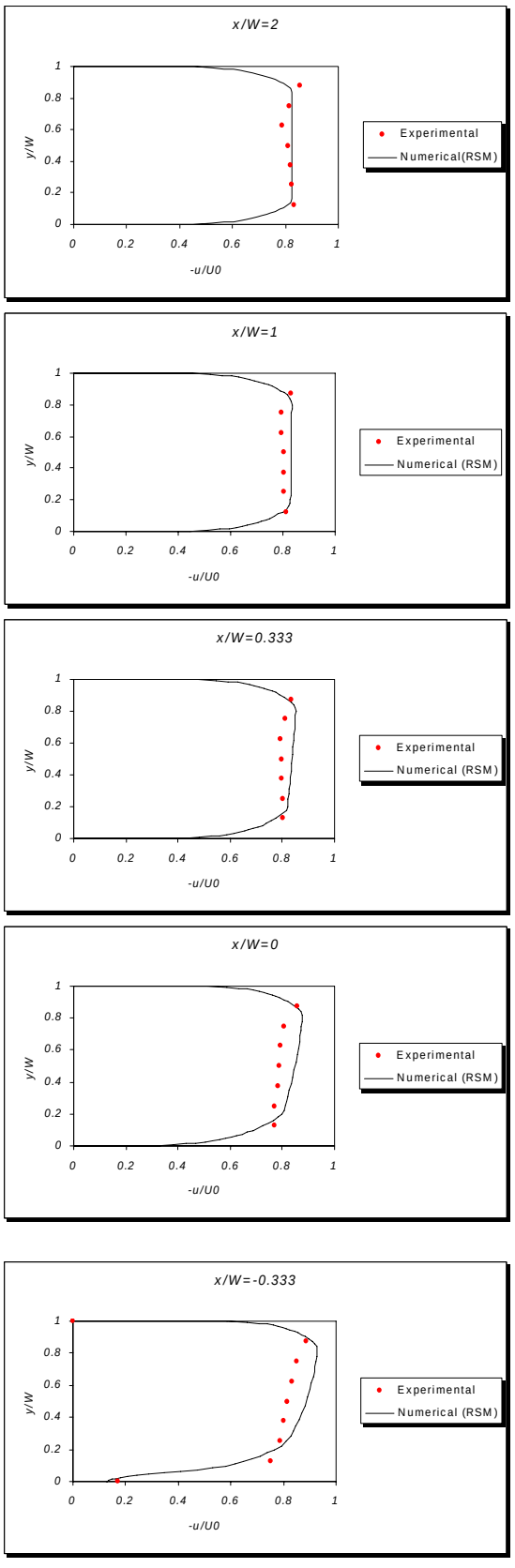

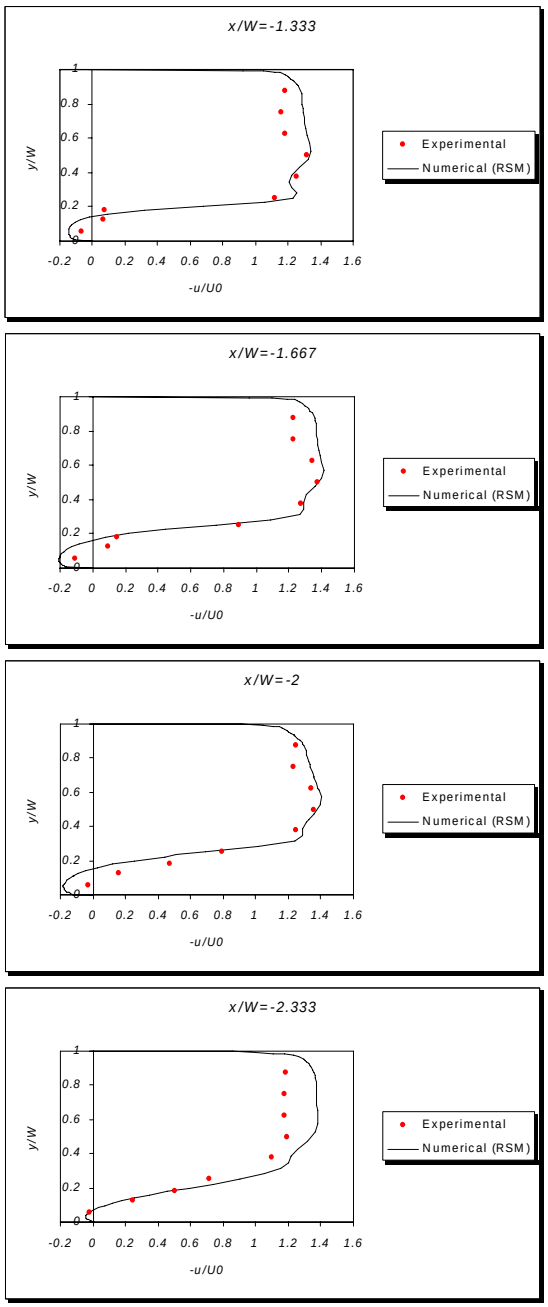

Fig. 3 Comparison of velocities in the main-channel with the experimental results close to the water surface

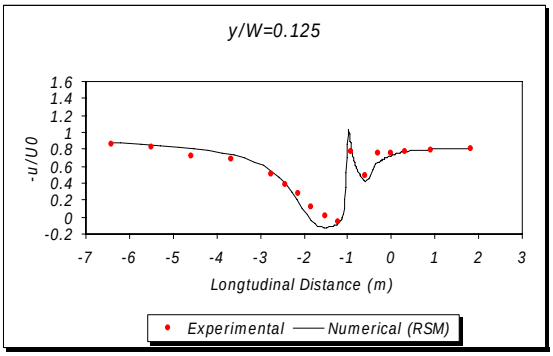

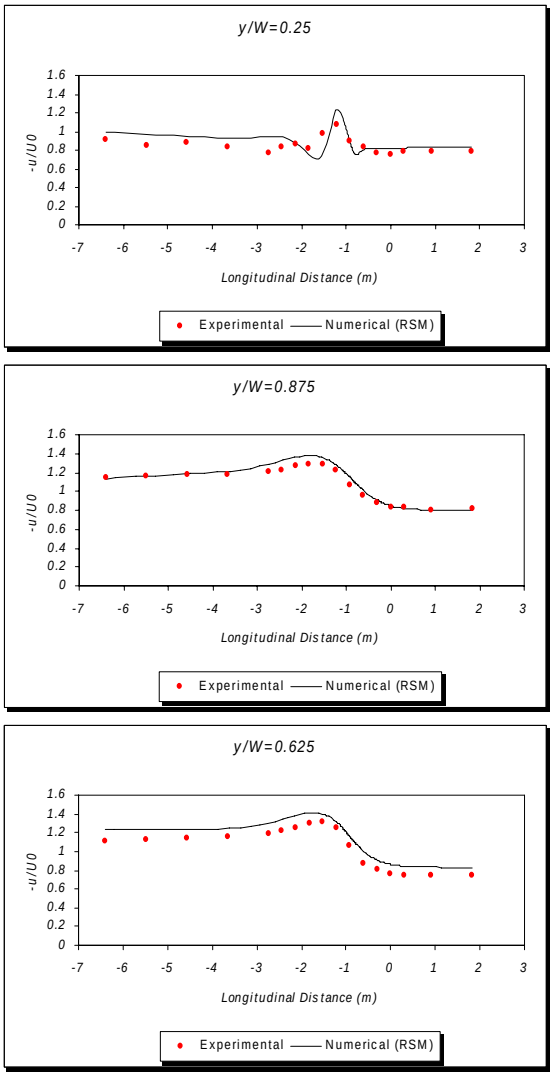

Fig. 4 Comparison of the velocity variation pattern along the main-channel reach with experimental results

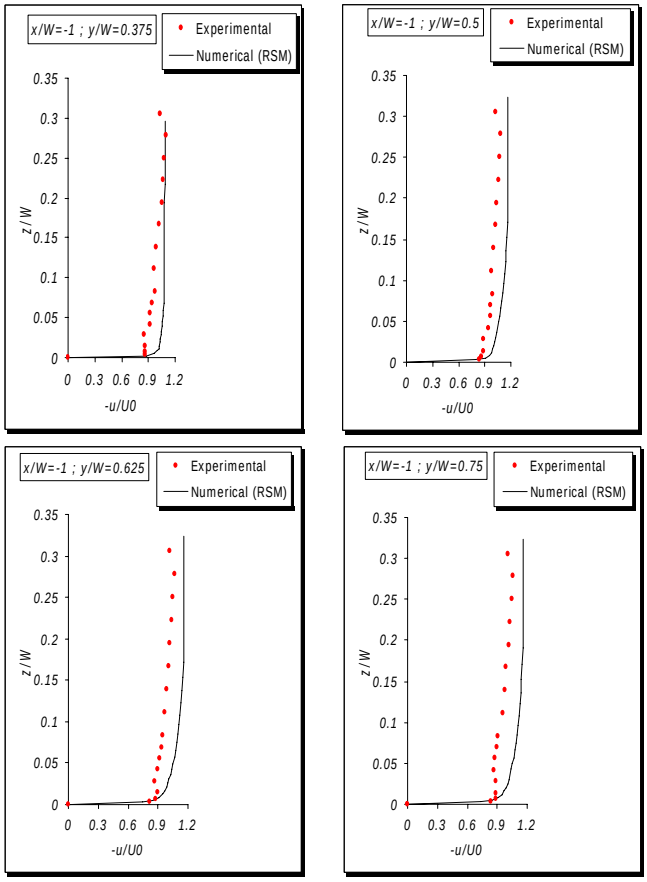

Fig. 5 Comparison of the vertical velocity profile at $x/W = -1$ with the experimental results

Comparison of the vertical velocity profile at ($x/W = -1$) with the experimental results indicates a close proximity between the estimated and experimental velocities (Fig. 5).

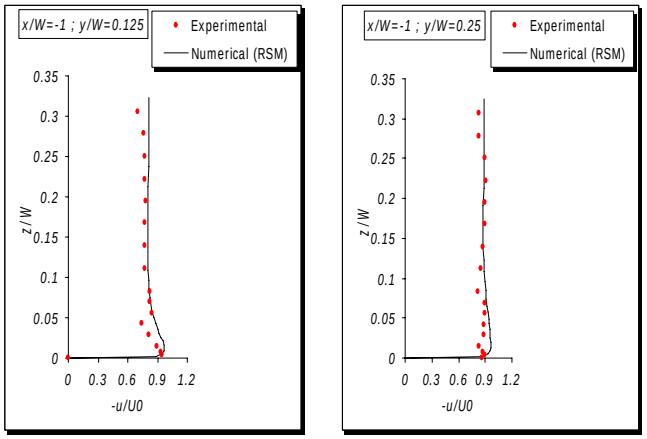

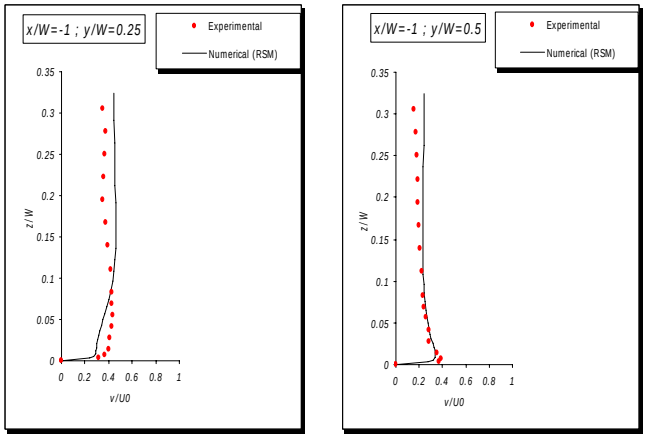

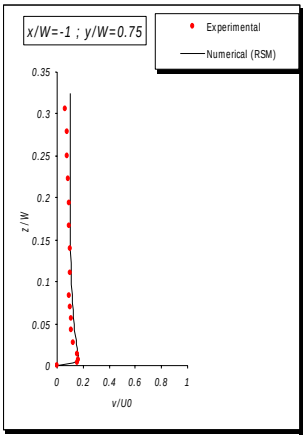

Fig. 5 Comparison of the vertical velocity profile at $x/W = -1$ with the experimental results(Continued)

From the comparisons of figure 6, it can be deducted that as the flow discharge ratio increases, the length and width of the separation zone generated in the main-channel, downstream of the flow confluence point, decreases.

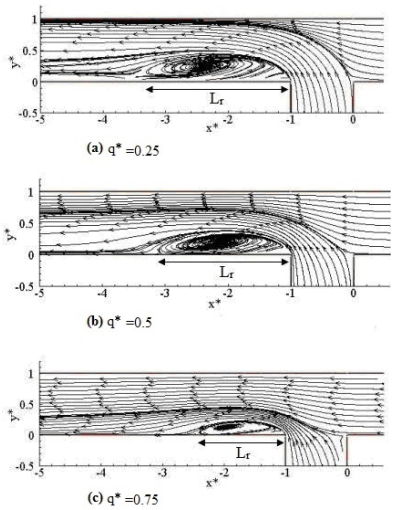

Fig. 6 Streamlines in the plane close to water surface

The reason is that any increases in the ratio of flow discharge in the main-channel to total discharge (q^*), there will be a corresponding increment in flow velocity and momentum of the main-channel but reduction of these in the side-channels.

The shape index of separation zone generated immediately after the confluence is compared with the experimental results [1], [7] which showed a relatively high proximity between the two sets of data (Fig. 7).

As can be observed from the results, the ratio of width to length of separation (shape index) showed an average quantity of 0.18. This average was observed by [1] and [7] to 0.19 and 0.17 respectively.

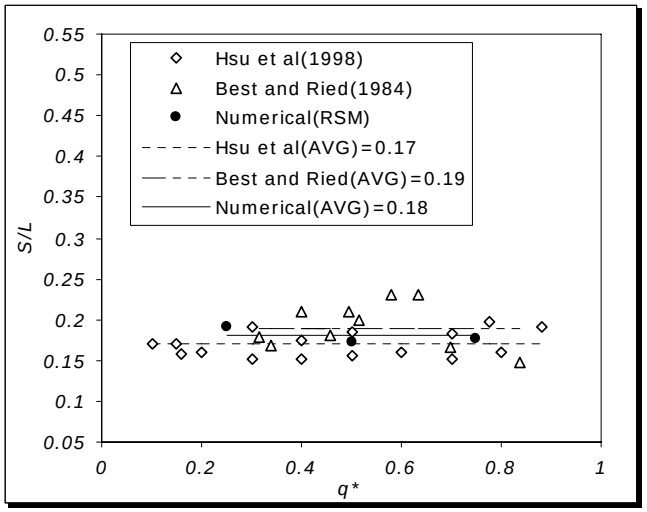

Fig. 7 Shape index of separation zone

NOTATION

u_i = Velocity components in Cartesian coordinates (u, v, w);
u = Cartesian velocity in x direction;
v = Cartesian velocity in y direction;
w = Cartesian velocity in z direction;
U_0 = Average velocity at downstream end of main-channel;
P = Total pressure;
ρ = Water density;
g_i = Gravity acceleration in Cartesian coordinate;
τ_{ij} = Stress tensor;
H_0 = Water depth at downstream end of main-channel;
W = Channel width;
D = Width of separation zone;
L = Length of separation zone;
Q = Total discharge;
q^* = Ratio of main-channel to total discharge;
F_r = Frude number $\left(= U_0 / \sqrt{gH_0}\right)$;
R_e = Reynolds number $\left(= \rho U_0 H_0 / \mu\right)$;
μ = Fluid viscosity;
P_{ij} = Production tensor;
ϕ_{ij} = Pressure-strain tensor;
D_{ij} = Diffusion tensor;
ε_{ij} = Dissipation tensor

REFERENCES

[1] Best, J.L. and Reid, I. (1984)."Separation zone at open-channel junction". Journal of Hydraulic Engineering. ASCE, 100(11), 1588-1594.
[2] Boyer, C., Roy, A.G., and Best, J.L. (2006)."Dynamics of a river channel confluence with discordant beds, flow turbulence, bed load sediment transport, and bed morphology". Journal of Geophysical Research-Earth, 111(F4), 1-22.
[3] De vriend, H.J. (1977)."A mathematical model in curved shallow channel". Journal of Hydraulic Research. 15(1).

[4] Ghobadian, R. (2006)."Investigation of flow, scouring and sedimentation at river-channel confluences". PhD thesis, Univ. of Shahid Chamran, Ahwaz, Iran.
[5] Gurram, S.K., Karki, K.S. and Hager, W.H. (1997)."Subcritical junction flow". Journal of Hydraulic Engineering. ASCE, 123(5), 447-455.
[6] Hager, W.H. (1989)."Transition flow in channel junctions". Journal of Hydraulic Engineering. ASCE, 115(2), 243-259.
[7] Hsu, C.C., Wu, F.S. and Lee, W.J. (1998a). "Flow at 90 equal-width open-channel junction." Journal of Hydraulic Engineering. ASCE, 124(88), 186-191.
[8] Lin, J.D. and Soong, H.K. (1979)."Junction losses in open-channel flows". Water Resource Research. Vol.15, No.1, pp.414-418.
[9] Rodi, W. (1979)."Turbulent models and their application in hydraulics-at state-of-the art review."IAHR, Delft, Netherlands.
[10] Shumate, E.D. (1998)."Experimental description of flow at an open-channel junction". Master thesis, Univ. of Iowa, Iowa.
[11] Taylor, E.H. (1944)."Flow characteristics at rectangular open-channel junction". Journal of Hydraulic Engineering. ASCE, 109, 893-912.